Spatial and temporal analysis of hillslope-channel coupling and implications for the longitudinal profile in a dryland basin

Katerina Michaelides[1,3*], Rory Hollings[1], Michael Bliss Singer[2,3], Mary H Nichols[4], Mark Nearing[4]

1 School of Geographical Sciences, University of Bristol, UK

2 School of Earth and Ocean Sciences, Cardiff University, UK

3 Earth Research Institute, University of California Santa Barbara, CA, USA

4 USDA ARS, Southwest Watershed Research Center, Tucson, Arizona, USA

* Corresponding Author

Abstract

The long-term evolution of channel longitudinal profiles within drainage basins is partly determined by the relative balance of hillslope sediment supply to channels and the evacuation of channel sediment. However, the lack of theoretical understanding of the physical processes of hillslope-channel coupling makes it challenging to determine whether hillslope sediment supply or channel sediment evacuation dominates over different timescales and how this balance affects bed elevation locally along the longitudinal profile. In this paper, we develop a framework for inferring the relative dominance of hillslope sediment supply to the channel versus channel sediment evacuation, over a range of temporal and spatial scales. The framework combines distinct local flow distributions on hillslopes and in the channel with surface grain-size distributions. We use these to compute local hydraulic stresses at various hillslope-channel coupling locations within the Walnut Gulch Experimental Watershed in SE Arizona, USA. These stresses are then assessed as a local net balance of geomorphic work between hillslopes and channel for a range of flow conditions generalising decadal historical records. Our analysis reveals that, although the magnitude of hydraulic stress in the channel is consistently higher than that on hillslopes, the product of stress magnitude and frequency results in a close balance between hillslope supply and channel evacuation for the most

This article has been accepted for publication and undergone full peer review but has not been through the copyediting, typesetting, pagination and proofreading process which may lead to differences between this version and the Version of Record. Please cite this article as doi: 10.1002/esp.4340

frequent flows. Only at less frequent, high-magnitude flows do channel hydraulic stresses exceed those on hillslopes, and channel evacuation dominates the net balance. This result suggests that WGEW exists mostly (~50% of the time) in an equilibrium condition of sediment balance between hillslopes and channels, which helps to explain the observed straight longitudinal profile. We illustrate how this balance can be upset by climate changes that differentially affect relative flow regimes on slopes and in channels. Such changes can push the long profile into a convex or concave condition.

1. Introduction

1.1 Rationale

The interaction between hillslopes and river channels plays a fundamental role in fluvial system evolution and in the storage and export of water and sediment. Hillslopes impose a sediment supply on river channels that is transported or stored, and which therefore impacts bed material grain size and local bed elevation (Attal and Lave, 2006, Korup, 2009, Michaelides and Singer, 2014, Singer and Michaelides, 2014, Sklar, et al., 2017). Channel behaviour in response to hillslope sediment supply depends on the mass and GSD of delivered sediment, its spatial and temporal characteristics (Benda and Dunne, 1997, Gabet and Dunne, 2003), as well as on the competence of the flow to transport the supplied sediment. Where hillslopes and channels are fully coupled (not buffered by a floodplain) (Bracken and Croke, 2007, Brunsden, 1993, Fryirs, et al., 2007, Harvey, 2001), sediment can be transported directly to the channel. If hillslope supply is greater than downstream channel transport, the result is net accumulation of sediment at that point, raising bed elevation. In contrast, if channel transport exceeds hillslope sediment supply, there will be net sediment evacuation and bed degradation.

Therefore, alluvial river bed elevation at a point along the longitudinal profile is determined by the net balance of sediment supply and channel sediment transport (Hack, 1957, Harvey, 2001, Leopold and Bull, 1979, Rice and Church, 1996, Simpson and Schlunegger, 2003, Singer, 2010, Slater and Singer, 2013). Sediment supply to any location in the channel is the sum of the contributions from upstream and from lateral sources. Over 10^1 – 10^3-yr timescales the divergence of sediment transport along the channel may be considered constant (Walling and Fang, 2003)

and lateral sources of sediment thus become significant in determining the net channel sediment balance. However, lateral sediment supply to the channel (e.g. from hillslopes) is poorly constrained in most river basins, which limits our understanding of its effect on this net balance, local bed elevation and by extension, its expression over the whole channel longitudinal profile (Tucker and Bras, 1998, Tucker and Slingerland, 1997, Willgoose, et al., 1991).

Over individual storm cycles, the balance between hillslope supply and channel transport controls changes in local sediment storage and bed elevation. Over centuries to millennia it governs longitudinal profile evolution (Snow and Slingerland, 1987). The prevailing climatic regime determines whether this balance is dominated by hillslope sediment supply (net channel accumulation) or channel sediment transport (net evacuation) over a particular timescale. For example, in basins with perennial channel discharge and slow subsurface storm flow through vegetated slopes, hillslope sediment supply only typically results from catastrophic slope failure, and the net balance along the channel profile favours channel sediment evacuation. However, in basins characterised by Hortonian overland flow on hillslopes and ephemeral flow in channels (i.e. dryland basins), the sediment balance between hillslopes and channels becomes more equivocal.

The longitudinal profile is therefore shaped by the relative magnitude and frequency of erosion events on hillslopes and in the channel over time (Wolman and Gerson, 1978, Wolman and Miller, 1960). A general question is whether more frequent sediment-moving events dominate the morphological expression in landscapes (Wolman and Miller, 1960), or whether topography is shaped by infrequent events that reorganize the landscape, followed by long period of ‘recovery’ (Baker, 1977, Wolman and Gerson, 1978). When considering hillslope sediment supply versus channel sediment evacuation, it is currently unknown whether channel events dominate over hillslope events and how the balance of geomorphic work in these two landscape components over the spectrum of runoff-producing rainstorms affects the shape of the long profile. In drylands, long profiles are often straight (Michaelides and Singer, 2014, Powell, et al., 2012, Singer and Michaelides, 2014, Vogel, 1989), suggesting that the balance between hillslope and channel erosional events differs from humid environments that display the typical concave-up equilibrium profile. In

dryland basins the stochasticity and spatio-temporal variability in rainfall (Singer and Michaelides, 2017) pose a challenge to anticipating the relative balance between hillslope and channel erosion.

1.2 Hillslope-channel coupling

Hillslope-channel coupling is particularly important for understanding the evolution of dryland basins for several reasons. 1) Overland flow during storms causes erosion of sparsely vegetated hillslopes that can deliver high and coarse sediment supply to the channel (Bull, 1997, Michaelides and Martin, 2012). 2) Spatial and temporal variability in rainfall means that hillslope sediment supply and channel evacuation may be out of phase such that one dominates the other over a particular timescale. 3) Channel sediment evacuation is accomplished by discrete flash floods travelling over dry streambeds with significant transmission losses (Hereford, 2002, Jaeger, et al., 2017).

These factors may result in net sediment accumulation in dryland channels as hillslope supply dominates over channel evacuation, except during rare, extreme events. Cycles of channel degradation or aggradation may persist in the landscape for decades to millennia (Bull, 1997, Slater and Singer, 2013, Slater, et al., 2015, Waters and Haynes, 2001), following changes in climate or base-level. However, due to the lack of theoretical understanding of the spatial and temporal expression of hillslope-channel coupling (Wainwright, et al., 2002), progressive changes in landscape topography are challenging to anticipate. In dryland basins that are particularly sensitive to climatic changes affecting runoff, we need a better understanding of hillslope-channel coupling to predict landscape responses and evolution to exogenous perturbations such as climate or base level change.

1.3 Hydrological and erosional processes in dryland basins

Dryland valleys are shaped by a cascading set of interacting processes that are triggered during individual rainstorms. Rainfall is converted to runoff by infiltration-excess overland flow on hillslopes, runoff erodes hillslope sediment, and this sediment is delivered to channels, some of which contributes to channel bed material. Runoff accumulates and generates flow in river channels, which in turn,

transports bed material sediment. However, storm events in drylands are short-lived and spatially discontinuous, leading to sporadic water and sediment delivery from hillslopes to channels. In these desert environments, the interaction between rainfall-runoff, vegetation, and erosion affects grain size of material eroded from slopes (Michaelides, et al., 2009, Michaelides, et al., 2012). In addition, channel flow undergoes significant transmission losses into the sedimentary bed such that flood discharge decreases with distance downstream and many floods do not reach the basin outlet (Renard and Keppel, 1966). These ephemeral channel flow processes in dryland basins leave a strong signal of inheritance from previous rainstorms, e.g., poorly sorted river beds lacking armouring (Laronne, et al., 1994), underdeveloped bar forms (Hassan, 2005), and generally simple topography (Singer and Michaelides, 2014). As channel transport rates are very sensitive to bed material GSDs, hillslope sediment supply may strongly influence subsequent channel sediment flux (Lekach and Schick, 1983) and thus, trends of sediment accumulation or evacuation in various parts of a dryland basin (Pelletier and DeLong, 2004).

The aim of this study is to investigate the net balance of hillslope sediment supply and channel sediment evacuation at distinct points along the channel, and to generalise this coupling within an entire river basin. Our analysis is based on the computation of a proxy for the net balance between sediment supply from hillslopes and channel sediment evacuation over a range of flows from the historical record. The spatial and temporal manifestation of this net balance can be used to understand long-term evolution of the longitudinal profile under the impact of past or future climatic conditions.

2. Study Site

The study was carried out at the Walnut Gulch Experimental Watershed (WGEW), a 149 km^2 basin near Tombstone, Arizona (AZ), USA (31° 43'N, 110° 41'W) (Figure 1). This basin, situated in the transition zone between the Chihuahuan and Sonoran Deserts, exists on a bajada sloping gently westwards from the Dragoon Mountains, reaching the San Pedro River at Fairbank, AZ. It is drained by Walnut Gulch, a sand and gravel-bedded ephemeral river. The climate of the region is semi-arid with low annual rainfall – average 312 mm yr^{-1} for the period 1956-2005 (Goodrich, et al., 2008). Convective thunderstorms during the summer monsoon season (July-

September) generate 60% of the annual precipitation and 90% of the runoff for WGEW and are the major driver of erosion and sediment redistribution (Nearing, et al., 2007, Nichols, et al., 2002, Nichols, et al., 2008, Osborn, 1983b, Osborn and Lane, 1969, Renard and Keppel, 1966). These storms are characterised by extreme spatial variability, limited areal extent, high intensity and short duration rainfall (Osborn, 1983a). It is not uncommon for storm events to exceed intensities of 100 mm hr^{-1} at the centre of the storm, lasting on the order of minutes (Nicholson, 2011, Renard and Laursen, 1975). During an event, channel flow decreases downstream due to transmission losses (Renard and Laursen, 1975). However, when considering the entire historical record of stream flow at various spatial scales within the basin, total annual discharge increases downstream (Figure 2A).

2.1 Existing Data

WGEW has the longest global record of runoff in a semi-arid site (Stone, et al., 2008) covering the period 1954-2015. Historical records of event discharge at WGEW exist for this period at 7 flumes along the main channel, and 7 on tributaries (Figures 1; 2A). Event based rainfall data exist for the same period at many of the 95 operational gauging stations across all of WGEW. (Goodrich, et al., 2008). These historical records of rainfall and discharge (http://www.tucson.ars.ag.gov/dap/) provide the opportunity to assess flow on hillslopes and in channels. A 1-m resolution Lidar DEM exists for WGEW obtained in 2007.

3. Methodology

3.1 Approach

The accurate assessment of sediment transport at high spatial resolution over a basin is logistically difficult without a time series of topographic surveys (e.g. repeat Lidar), widespread measurements of sediment flux and/or erosion rates from geochronology. To better understand the spatial variability of hillslope-channel coupling, we compute hydraulic stress (i.e. the force applied to a substrate by flowing water) acting upon a template of measured surface grain size distributions as a proxy for potential sediment transport. We employ a rich historical record of rainstorm intensity and duration data and discharge measurements at various spatial scales in WGEW to extract characteristic values of flow in the channel and on the

hillslopes for the stress calculations. We then multiply hillslope and channel stress metrics by the frequency of their occurrence in the historical record to generate a proxy for geomorphic work done by each flow. The net balance of these frequency-normalised stresses can be used as a comparison of relative sediment yield proxies, to infer local hillslope-channel coupling as the relative dominance of hillslope sediment supply or channel sediment evacuation. Finally, we generalise this analysis to assess the likely impact of hillslope-channel coupling over the last several decades on the longitudinal profile of Walnut Gulch.

3.2 Ingredients for analysis

Our subsequent analyses use the following data obtained from the historical records in WGEW and a field campaign: decadal records of event rainfall, decadal records of event discharge, hillslope and channel grain size measurements and topographic data. The rainfall data are used as inputs into a rainfall-runoff model to produce values of hillslope runoff. The 1-m Lidar DEM was used to calculate a flow accumulation raster in ArcGIS, from which upstream drainage areas for each transect were computed. Rainfall and channel discharge data were used in the calculation of hydraulic stress magnitudes and probabilities (frequencies).

3.3 Field Measurements of topography and grain size

We measured topography and grain sizes in the field to provide relevant information as input for calculating hydraulic stresses (Eq 1). We surveyed by real time kinematic GPS (accuracy: 1 cm vertically; 2 cm horizontally) channel centreline elevations at 72 locations spanning ~30 km of the drainage network. At a subset of 31 locations we measured channel width and adjacent hillslope profiles, of which 11 were fully coupled on both sides and 20 were partly coupled (hillslope-channel connection only on one side of the channel) – giving a total of 42 hillslopes. Channel measurements were made at intervals of ~100 m in the headwaters and at ~500 m downstream (Figure 1). The local channel slope, *S*, at each transect was computed as:

$$S = \frac{\left(\frac{z_{j-1}-z_j}{x_j-x_{j-1}}\right)+\left(\frac{z_j-z_{j+1}}{x_{j+1}-x_j}\right)}{2} \quad (1)$$

in which z is centreline elevation, x is distance downstream, and j is the location identity. Channel slope in this basin is insensitive to sampling resolution, since the longitudinal profile is essentially straight. We have confirmed this by comparing slope obtained from 1-m, 10-m, and 30-m elevation data for WGEW.

We measured grain size of surface sediments at three locations on each of the 44 hillslopes and at 81 locations in the channel. A photographic method was used for grain size analysis (Buscombe, et al., 2010). Photographs of the surface were taken using a Nikon Coolpix S9700 16.0-megapixel (4608 x 3456 pixels) digital camera mounted to a survey pole at a height of approximately 25 cm and orthogonal to the ground under natural light. The camera was set to automatically reduce shake. A scale was placed in the field-of-view of all photographs near to the edge of image. The image resolution varied between photos because modifications were needed to the apparatus to ensure that the photo was orthogonal to the ground and without shadows cast by the apparatus or nearby vegetation. The camera height therefore varied approximately ±0.15 m, resulting in image resolutions of approximately 0.1 mm/pixel in all photos. We employed an automated method of grain size distribution detection (Buscombe, 2013, Buscombe, et al., 2010).

This method was tested against a surface pebble count method for phi grain size classes between 2 mm and 512 mm using the Wolman method (Wolman, 1954). A selection of grain size distributions derived by both methods were compared and found to be statistically similar (Supplementary Table 1). Photographically derived grain size distributions were analysed using GRADISTAT software (Blott and Pye, 2001) to generate characteristic size percentiles (D_{10}, D_{50} and D_{90}).

3.4 Magnitude of hydraulic stress

We use stream power instead of shear stress as a metric of hydraulic stress, as it minimises data requirements and enables direct comparison of stress on hillslopes and in channels. Additionally, shear stress has been shown to be a poor predictor of sediment transport by overland flow on coarse-mantled desert hillslopes (Abrahams, et al., 1988). Stream power incorporates both runoff depth and velocity of the flow, which co-vary on hillslopes to affect sediment entrainment (Michaelides and Martin, 2012), so it is a more sensible metric of hydraulic stress in this context. While runoff

depth and velocity measurements are not common, information on depth and velocity can be easily obtained from rainfall-runoff models in Hortonian overland flow environments (Michaelides and Wainwright, 2002), where event-based rainfall data are available.

Stream power (W/m) is defined as the product of discharge, slope, and weight of water:

$$\Omega = \rho g Q S \quad (2)$$

where ρ is the density of water (1000 kg/m^3 at 4°C), g is gravity (9.81 m/s^2), Q (m^3/s) is discharge, and S is energy gradient (m/m), which is equivalent to the bed slope for uniform flow. Normalising by width (for channels), we obtain unit stream power, ω (W/m^2):

$$\omega = \rho g Q S / B \quad (3)$$

where B is the width of flow (m). Discharge for a rectangular cross section of channel is defined as:

$$Q = UBh \quad (4)$$

Where U is mean stream velocity (m/s) and h is flow depth (m). Therefore, we can rewrite (Eq 3), replacing Q with its components as:

$$\omega = \rho g h S U \quad (5)$$

Eq 5 can be applied to the channel by inverting discharge data with Eq 4, again assuming a rectangular cross section, which is a common feature of dryland channels (Leopold, et al., 1966, Singer and Michaelides, 2014). It is applied to the hillslope using flow velocity, depth and discharge output from a rainfall-runoff model where, $q = uh$, and q is unit hillslope discharge (m^2/s), h is overland flow depth (m), and u is downslope velocity (m/s) (Michaelides and Wainwright, 2002).

Parker (1979) defined dimensionless depth ($h^* = h/D_{50}$) and velocity ($V^* = U/\sqrt{gRD_{50}}$), where R is the submerged specific gravity of the sediment, $R = (\rho_s - \rho)/\rho$, ρ_s is sediment density and D_{50} is the median diameter of the surface sediment from field measurements. Eaton and Church (2011) combined *h** and *V** with a dimensionless slope term ($S^* = \rho gS/\rho gR$) to derive dimensionless stream power as $\omega^* = h^*V^*S^*$. After combining and simplifying, dimensionless stream power can be expressed as:

$$\omega^* = \frac{\omega}{\rho[gRD_{50}]^{3/2}} \quad (6)$$

Using this metric (*ω**), we can compare the relative magnitudes of hydraulic stress for the channel and adjacent hillslopes for any percentile of flow.

3.5 Hydraulic stress calculations

3.5.1 Channel

We retrieved from the online database information on discharge at each flume including runoff event start-time, duration (mins), total equivalent runoff depth (mm), and the peak runoff rate (mm/hr) for each discharge event measured at every flume in WGEW since 1953. We extracted discharge values for 25th, 50th and 75th percentiles for 6 of the flumes to represent the low, medium and high discharges. These were plotted against drainage area on a log-log plot and a linear regression line was drawn between the points (Figure 2A). Using these regression equations, we calculated discharge values for each flow percentile for each transect location in the channel (Figure 1) as a function of the upstream contributing area. Based on local discharge values generated by the relationship between discharge and drainage area we then computed *ω* by (Eq 5) and *ω** by (Eq 6) for each transect location.

3.5.2 Hillslopes

Hillslope runoff is not measured directly in a systematic way, so we employed a rainfall-runoff model to convert measured rainfall events into runoff events utilising

the 63-year historic record of rainfall in WGEW. We plotted the event rainfall intensity versus duration for every storm on record at all rain gauges in WGEW. We then thresholded this dataset at an intensity of 15 mm/hr (Figure 3A), as a conservative estimate of the intensity above which runoff is generated. This threshold was based on a various values from previous work in this basin (Osborn and Lane, 1969, Syed, et al., 2003). Figure 3B and 3C show the distributions of rainfall intensities and durations over all recorded events above 15mm/hr.

We then used the STOchastic Rainfall Model (STORM, (Singer and Michaelides, 2017)) to randomly sample rainfall events from this thresholded phase space of intensity-duration, such that a randomly selected value of total rainfall for each year is satisfied across the basin. Thus, these simulations are faithful to the hydroclimate of WGEW. We simulated three ensembles each of 30 years to broadly represent the range of rainstorms recorded at Walnut Gulch over the last several decades.

To convert these rainfall events into hillslope runoff, we employed the rainfall-runoff model COUP2D (Michaelides and Martin, 2012, Michaelides and Wainwright, 2002, Michaelides and Wainwright, 2008, Michaelides and Wilson, 2007), which simulates overland flow hydraulics on hillslopes in response to discrete rainfall event inputs. Because runoff response to rainfall is significantly modulated by hillslope length (e.g. see Michaelides and Martin, 2012), we ran model simulations (using the same randomly selected rainfall events) on four hillslope lengths: 25, 50, 75 and 100 m to give us the signal of rainfall to runoff for different hillslope lengths (total simulations = 1832). Hillslope angle is important for determining the flow hydraulics (i.e. the depth-velocity split) but, for the same infiltration rate it does not affect the discharge, so we used a constant angle in our simulations (10°). We also used a constant value of Manning's *n* (0.056) in these ensemble model simulations. The distribution of all modelled runoff values is shown in Figure 3D.

We then used the modelled *q* values to calculate flow percentiles (25^{th}, 50^{th} and 75^{th}) for each hillslope length. These values of flow percentile were plotted against hillslope length and a power law function was the best fit between the points (Figure 3E). Using these equations, we calculated discharge for each flow percentile for each of the 44 hillslopes along the sampling transect (Figure 1 and Supplementary

Table 2) as a function of the hillslope length which was then used to computed hillslope ω by (Eq 5) and hillslope ω^* by (Eq 6).

COUP2D simulates infiltration-excess and saturation-excess overland flow as a result of filling a fixed soil moisture store and infiltration is represented using the modified Green and Ampt (1911) infiltration model (Michaelides and Wilson, 2007). Runoff is routed on a 2D rectangular grid of a hillslope strip (hillslope length x 2 m width) using the kinematic wave approximation. This approximation is rated using the Manning's n friction factor, with flow routing from cell to cell defined by a steepest descent algorithm.

For simplicity we use one value of initial and final infiltration rates (2.2 mm and 0.25 mm/min respectively) for the model simulations based on reported measurements by Abrahams, et al. (1995) in WGEW. While we acknowledge that infiltration rates on hillslopes are highly variable, model sensitivity analysis has shown that rainfall rate is by far the most important determinant of runoff rates compared to infiltration rates (see Michaelides and Wainwright, 2002) and spatial variability in infiltration rates is only important where the runoff magnitude is low (i.e. rainfall and infiltration rates are similar). Even then, the sensitivity of runoff rates to spatial patterns in infiltration is relatively low (see Michaelides and Wilson, 2007). All hillslope variables are provided in Supplementary Table 2.

3.6 Probability of hydraulic stress occurrence

To assess the net balance of hydraulic stress over a multidecadal period, we normalise the magnitude of each value of the driving flow (q on hillslopes and Q in channels) by the probability (frequency) of its flow occurrence in the historical record to produce the computed value of ω^*. We separately compute probabilities of occurrence for hillslope runoff and channel discharge.

3.6.1 Channel

In the channel, we calculate an exceedance probability for streamflow equalling or exceeding a particular value of channel discharge, Q (m^3/s) as:

$$p(Q_{xx}) = \frac{\sum_{k=1}^{f}\left[\frac{(\#events \geq Q_{xx}}{\#\ storm\ \ days\ \ at\ k}\right]}{f} \quad (7)$$

where *k* is a flume identifier, *f* is the total number of flumes used (n=7), and subscript *xx* indicates the percentile of discharge (25th, 50th, 75th). In other words, we are computing the overall channel flow probability of occurrence as the average of all local (at each flume) channel probabilities of *Q* exceeding a particular value. In this case, we multiplied average of storm days per year by the number of years of record for each flume to obtain the total # of storm days in (Eq 7).

3.6.2 Hillslopes

On hillslopes, we calculate the probability of runoff occurrence equalling or exceeding a particular value of hillslope runoff, *q* as:

$$p(q_{xx}) = \frac{(\#events \geq q_{(xx)})}{\#storms} \quad (8)$$

where *q* indicates hillslope unit runoff (m^2/s) and subscript *xx* indicates the percentile of runoff (25th, 50th, 75th). Based on a characterisation of the rainfall record, we computed an average of 37 rainstorms per year in WGEW (Singer and Michaelides, 2017), yielding 1110 storm events over 30 years (used in the denominator of Eq 8).

3.7 A proxy for geomorphic work

The magnitude of stress produced by a flow scaled by its likelihood describes its geomorphic effectiveness in shaping the landscape over longer timescales (Wolman and Miller, 1960). Thus, we compute a proxy for geomorphic work (*Λ*) done for each percentile of stress on either the hillslope or in the channel by multiplying (Eq 6) by either (Eq 7) or (Eq 8) as:

$$\Lambda\_\mathrm{HS}_{xx} = \omega^*\_HS_{xx}.p(q_{xx}) \quad (9)$$

and

$$\Lambda\_\mathrm{CH}_{xx} = \omega^*\_CH_{xx}.p(Q_{xx}) \quad (10)$$

for the hillslopes and channel, respectively.

3.8 Quantifying geomorphic work balance at WGEW

For the hillslope and channel at each transect, we multiplied all ω^* values calculated for each percentile magnitude by the probability of q or Q exceeding or equalling its respective magnitude, given by equation (7) and (8) to generate Λ_HS_{xx} and Λ_CH_{xx} (Eqs 9 and 10), respectively. We then calculated the net local balance (N_{Bal}) between hillslope and channel Λ at each hillslope-channel transect for paired values of Λ_HS_{xx} and Λ_CH_{xx} at each topographic cross-section along the channel as:

$$N_{Bal} = \Lambda\_\mathrm{HS}_{xx} - \Lambda\_\mathrm{CH}_{xx} \quad (11)$$

N_{Bal} therefore, provides an indirect assessment of the localised balance between the sediment supply from hillslopes to the channel and channel sediment evacuation. A positive value of N_{Bal} indicates locally higher supply by hillslopes, whereas a negative value suggests net evacuation of supplied sediment. Over longer timescales, positive values of N_{Bal} along the entire channel would produce a convex long profile, and negative N_{Bal} values would generate a concave up profile. Where are fully coupled hillslopes on both sides of the channel for any particular transect, Λ_HS includes the additive contributions from both.

4. Results

4.1 Morphological and sedimentary characteristics from field measurements

The field data reveal a straight longitudinal profile in the channel, where elevation monotonically declines downstream, with minimal impact of tributaries (Figure 4A). The straight long profile is consistent with previous work in drylands (Michaelides and Singer, 2014), but which has yet to be fully explained from a mass balance perspective. Channel width fluctuates and displays no downstream trend (Figure 4B), which is again consistent with other dryland basins (Jaeger, et al., 2017, Michaelides and Singer, 2014) and may reflect a topographic expression of downstream transmission losses. Hillslope angles throughout WGEW are low (median = 5.7°; IQR = 2.9˚), and 90% of the measured slopes have angles <10°

(Figure 5A). Hillslope lengths vary greatly across our surveyed transects (median = 149.7 m; IQR = 131.5 m) (Figure 5B).

Characteristic grain sizes in the channel and on hillslopes fluctuate with no downstream fining trend (Figure 4C). Hillslope surface sediments are generally coarser than channel bed material sediment and there was no spatial correlation between the hillslope and channel GSD. However, we found that over all sites analysed the hillslope D_{50} and channel D_{90} are statistically similar (Kolmogorov-Smirnov statistic (KS) = 0.1844, p = 0.2842, n1/n2 = 71/44). This result is consistent with findings from another dryland environment, which suggested that sediment delivered from slopes to channels in drylands becomes the characteristic scale of hydraulic roughness (Michaelides and Singer, 2014, Singer and Michaelides, 2014).

Figure 5C displays the aggregated channel and hillslope GSDs over nested drainage areas within the watershed. This analysis reveals that hillslope surface sediment GSD is scale invariant, despite variability in slope length and angles (Figure 5A and 5B). In contrast, the channel GSDs display a coarsening trend with increasing contributing area. This finding contradicts most published channel sediment data which display downstream fining (Ferguson, et al., 1996, Menting, et al., 2015, Sternberg, 1875), but is consistent with some published work where sediment supply exceeds channel transport (Brummer and Montgomery, 2003) or where flow competence causes a winnowing of fines (Attal, et al., 2015, Singer, 2010).

4.2 Hydraulic stress analysis

4.2.1 General analysis of ω^* and Λ

Figure 6 compares the distributions of ω^*, p and Λ between hillslopes and the channel calculated from the entire dataset (all flow percentiles and all transects). Figure 6A shows that dimensionless stream power (ω^*) in the channel is significantly higher than on the hillslopes (KS = 0.77, $p = 9.5 \times 10^{-44}$, n1/n2 = 207/135). In contrast, the probabilities of occurrence (p) associated with these stresses are significantly higher for the hillslope than for the channel (KS = 0.61, $p = 4.8 \times 10^{-3}$, n1/n2 = 18/12*)* (Figure 6B). The product of the stress and associated probability, Λ, is significantly greater in the channel than on the hillslopes albeit they converge to being much closer in value (KS = 0.59, $p = 3.1 \times 10^{-25}$, n1/n2 = 207/135). This suggests that N_{Bal}

should be slightly negative overall. In other words, dimensionless stream power is found to be an order of magnitude greater in the channel than on hillslopes. Even when accounting for the higher probabilities of these stream powers occurring on the hillslopes than in the channel, the net effect in terms of potential geomorphic work is that the channel overall does more work than the hillslopes.

Figure 7 presents comparisons of ω^*, p and Λ between hillslopes and the channel organised by flow percentiles (Q_{xx} and q_{xx}). Figure 7A shows that ω^*_CH is systematically and significantly higher than ω^*_HS for all percentiles of flow (Supplementary Table 3). However, the probabilities of hillslope $p(q)$ and channel $p(Q)$ hydraulic stress occurrence, show the reverse pattern and are systematically and significantly higher for hillslope flows than channel flows across all flow percentiles (Figure 7B; Supplementary Table 3).

The product of the hydraulic stresses and their respective probabilities yields a metric of geomorphic work (Λ) that indicates a tendency towards sediment transport. At the lowest and highest flow percentiles (25^{th} and 75^{th}) the channel has higher Λ values than the hillslope – meaning that channel sediment transport exceeds hillslope sediment supply to the channel under those flow conditions. However, at median flow conditions (50^{th} percentile) hillslope Λ exceeds that of the channel, suggesting that under the most commonly occurring flow conditions, hillslope sediment supply exceeds channel sediment evacuation. The differences between hillslope and channel Λ values are statistically significant across all flow percentiles (Supplementary Table 3).

The higher probability of all flows on hillslopes counterbalances the higher stream power in the channel, resulting in close balance between the potential geomorphic work in the two landscape components especially at the median flow conditions. At the high flow percentiles, which occur less frequently, the channel dominates over the hillslopes.

4.2.2 Net balance of geomorphic work (N_{Bal})

Figure 8 presents N_{Bal} (Eq 11) against drainage area based on keeping Λ_CH_{xx} constant and subtracting it from the three values of Λ_HS_{xx} (for xx = 25, 50, 75). In

other words, the variability in N_{Bal} at each transect is a function of the range of hillslope runoff values. At lower drainage areas (<4 km^2) and over all flow percentiles, N_{Bal} is positive indicating the dominance of hillslope sediment supply at these scales. As drainage area increases, N_{Bal} tends to fluctuate around zero but becoming more negative as flow percentile increases (blue to red, Figures 8A-C). Overall, at low flow percentiles, the hillslopes dominate at all scales, whereas at median and high flows hillslopes and channels are more in balance.

Figures 8D-F present the distributions of N_{Bal} values aggregated for various spatial scales throughout the basin corresponding to Figures 8A-C. At the headwater basin scale (<4 km^2), the median N_{Bal} is positive for each flow percentile but the range spans positive and negative values. At the intermediate scale (4-40 km^2) N_{Bal} is the most negative of all the scales. Across all streamflow percentiles, median N_{Bal} values at the whole basin scale (149 km^2) are very close to zero. This result suggests an approximate balance between hillslope supply and channel evacuation over the basin.

Figure 9 presents N_{Bal} against drainage area based on keeping Λ_HS_{xx} constant and subtracting from it from the three values of Λ_CH_{xx} (for xx = 25, 50, 75) – the inverse case from Figure 8. In this case, the variability in N_{Bal} at each transect is now a function of the range of channel discharge values. The trend in N_{Bal} with drainage area in this case is different to Figure 8A-C. At low (25th) and high (75th) hillslope flows, the balance is clearly dominated by channel sediment evacuation at all spatial scales (Figure 9A and 9C). At the 50th hillslope flow percentile this trend is reversed, and the balance is tipped in favour of hillslope sediment supply at most spatial scales. This is mirrored in Figures 9D-F which clearly shows negative N_{Bal} values at q_{25} and q_{75}, and positive N_{Bal} values at q_{50}, across all spatial scales.

5. Discussion

This analysis revealed that the magnitude of ω^*_CH is consistently higher than ω^*_HS, regardless of flow percentile (Figure 7A). However, once we multiplied these stress magnitudes by their respective frequency of occurrences in the historical hydrological record at WGEW, we find variations in the resulting geomorphic work

metric (N_{Bal}) between the flow percentiles that flip between channel dominance to hillslope dominance. Particularly, at the low and high flow percentiles (25^{th} and 75^{th}) channel geomorphic work tends to be higher than that of the hillslopes. However, at the 50^{th} flow percentile, hillslope geomorphic work exceeds that of the channel (Figure 7C), a result that corroborates measurements in a first order sub-basin of WGEW showing hillslopes to be the dominant contributor to total sediment yield (Nichols, et al., 2013). This result suggests that WGEW exists mostly (~50% of the time) in this condition of hydraulic stress balance between hillslopes and channels. Furthermore, the net local balance that is struck between these frequency-normalised stresses (N_{Bal}) on hillslopes and channels over the entire basin fluctuates around zero, over all spatial scales and over all recorded flows (Figures 8 and 9).

In this paper, we revealed longitudinal variations in N_{Bal}, which depend on both the magnitude and frequency of driving flow events (Figure 8 and 9). Specifically, we interpret from these stress metrics and the flow probabilities that the common condition of this dryland landscape is one of infrequent flow in the channel and more frequent overland flow on slopes for the same rainfall events (Figure 6B). However, when the channel does flow at higher than average levels (<25% of the time), channel hydraulic stress systematically exceeds that on adjacent hillslopes. Thus, it appears that the channel of WGEW operates under a regime of net sediment accumulation from hillslopes most of the time, followed by (less frequent) episodic transport of channel sediment.

Channel flows, however, are not generally long-lived enough to evacuate all the sediment supplied by hillslopes, especially considering that discharge declines in the downstream direction due to transmission losses (Renard and Keppel, 1966). Instead, ephemeral channels incompletely sort the supplied hillslope sediment into diffuse coarse and fine patches that fluctuate down the channel (Figure 4B and 4C), in a manner that is typically out of phase with hillslope-channel coupling loci and width fluctuations (Michaelides and Singer, 2014, Singer and Michaelides, 2014)). Thus, the WGEW channel apparently inherits coarse patches from the bounding hillslopes and they accumulate such that the GSD coarsens with increasing drainage area (Figure 5C). The coarse particles delivered from hillslopes become the

hydraulic roughness of the channel (Michaelides and Singer, 2014), limiting river incision under moderate flow conditions.

Since the balance between hillslope sediment supply and channel sediment evacuation (N_{Bal}) exerts an important control on local channel bed elevation (Figure 10A-C), we may infer that a net zero balance struck over a long enough time period (e.g. at least several decades) would produce a long profile that does not change appreciably in elevation (Leopold and Bull, 1979). While fluctuations in local bed elevations would be expected, there would be no long-term trend of aggradation or degradation, a condition supported by previous dryland research (Leopold, et al., 1966, Powell, et al., 2007). This idea is distinct from that of the graded river profile, where the river transports all the sediment supplied to it because of supply limitation (Leopold and Bull, 1979, Mackin, 1948). By contrast, a dryland system such as WGEW appears to have a very high supply of sediment that has likely persisted as long as the duration of the current hydrological regime. Ephemeral channels such as WGEW can thus be considered oversupplied with sediment, which are shaped by infrequent and discontinuous channel flow into a straight longitudinal profile and symmetrical channel cross sections (referred to as 'topographic simplicity', (Singer and Michaelides, 2014)). This interpretation of the equilibrium condition for ephemeral channels is consistent with observations in other dryland environments (Hassan, 2005, Leopold, et al., 1966, Powell, et al., 2012, Vogel, 1989) and with modelling of long profile development under different forcing conditions (Snow and Slingerland, 1987). This is a topic of ongoing research, so the first-order mechanisms driving this topographic condition have not yet been determined.

One might wonder how stable a straight long profile might be and how it might be perturbed into becoming concave or convex. Modelling of long profile evolution might help to address such questions. However, our spatially explicit analysis linking magnitude (ω^*) and frequency (p) of hydraulic stresses suggests that climate change could have important consequences for the long profile. While the pdfs of the product of magnitude and frequency (Λ) for hillslopes and channels have limited overlap under the current hydrological regime at WGEW, these distributions could shift toward or away from each other, depending on how climate change is expressed in runoff regimes. Singer and Michaelides (2017) analysed historical hydrological

trends at WGEW and found that rainfall intensity has declined significantly in recent decades and especially for high intensity rainfall (>15 mm/hr), yet total monsoonal rainfall is trending upward over this same time period. This has translated into a significant downward trend in runoff at the WGEW basin outlet (Singer and Michaelides, 2017). These findings suggest that there are more storms each monsoon delivering less intense rainfall, which would tend to increase the frequency of hillslope runoff and decrease the frequency of channel streamflow (Figure 10D). If this climate change trend persists well into the future, it would tend to maintain a straight long profile, but could even yield a convex long profile by oversupplying the channel with sediment that is not evacuated (Figure 10E). Indeed, there is some evidence for a trend of oversupply from repeat channel cross sections over multiple decades (Supplementary Figure A). However, it is worth noting that dryland environments often experience dry periods that are punctuated by catastrophic flooding, wherein the system can reset itself with hydraulic stresses in the channel that are large enough to cross a geomorphic threshold and ream out stored sediment (Baker, 1977, Baker, 1987, Singer and Michaelides, 2014, Wolman and Gerson, 1978).

6. Conclusions

We developed a framework for analysing the relative balance between hillslope sediment supply to the channel and channel sediment evacuation, over a range of temporal and spatial scales in a dryland basin, where erosional processes are driven by the flow of water. Our approach utilises historical records of rainfall and streamflows in combination with surface grain-size distributions, to compute local hydraulic stresses at 32 hillslope-channel transects. The magnitude of these stresses was multiplied by the frequency of their occurrence in the historical record to produce a proxy for geomorphic work. We then assessed the local net balance between hillslope and channel ‘geomorphic work’ at each transect over a range of flow conditions generalising decadal historical records. Our results reveal that overall there is a close balance between hillslope supply and channel evacuation for high frequency flows. Only at less frequent, high-magnitude flows does channel ‘geomorphic work’ exceed that of hillslopes, and channel evacuation dominates the net balance. While there are spatial patterns in the net balance, they tend to cancel out yielding an overall basin-scale balance that is close to zero. This result suggests

that WGEW exists mostly (~50% of the time) in an equilibrium condition of balance between hillslopes and channels, which helps to explain the straight longitudinal profile. We also demonstrate that climate changes can affect this net balance and thus change the shape of the longitudinal profile.

Acknowledgements
This work was part funded by a NERC studentship to RH. Rosie Lane provided some Matlab code. Field support at WGEW was provided by various staff at ARS-USDA in Tucson.

References

Abrahams AD, Parsons AJ, Luk SH. 1988. Hydrologic and sediment responses to simulated rainfall on desert hillslope in Southern Arizona CATENA **15**: 103-117. DOI: 10.1016/0341-8162(88)90022-7

Abrahams AD, Parsons AJ, Wainwright J. 1995. Effects of vegetation change on interrill runoff and erosion, Walnut Gulch, southern Arizona. Geomorphology **13**: 37-48. DOI: http://dx.doi.org/10.1016/0169-555X(95)00027-3

Attal M, Lave J. 2006. Changes of bedload characteristics along the Marsyandi River (central Nepal): Implications for understanding hillslope sediment supply, sediment load evolution along fluvial networks, and denudation in active orogenic belts. In *Tectonics, Climate, and Landscape Evolution*, Willett SD, Hovius N, Brandon MT, Fisher DM (eds). Geological Soc Amer Inc: Boulder; 143-171.

Attal M, Mudd SM, Hurst MD, Weinman B, Yoo K, Naylor M. 2015. Impact of change in erosion rate and landscape steepness on hillslope and fluvial sediments grain size in the Feather River basin (Sierra Nevada, California). Earth Surf. Dynam. **3**: 201-222. DOI: 10.5194/esurf-3-201-2015

Baker VR. 1977. Stream-channel response to floods, with examples from Central Texas. Geological Society of America Bulletin **88**: 1057-1071

Baker VR. 1987. Paleoflood hydrology and extraordinary events. Journal of Hydrology **96**: 79-99

Benda L, Dunne T. 1997. Stochastic forcing of sediment supply to channel networks from landsliding and debris flow. Water Resources Research **33**: 2849-2863

Blott SJ, Pye K. 2001. GRADISTAT: a grain size distribution and statistics package for the analysis of unconsolidated sediments. Earth Surface Processes and Landforms **26**: 1237-1248

Bracken LJ, Croke J. 2007. The concept of hydrological connectivity and its contribution to understanding runoff-dominated geomorphic systems. Hydrological Processes **21**: 1749-1763

Brummer CJ, Montgomery DR. 2003. Downstream coarsening in headwater channels. Water Resources Research **39**: 14. DOI: 1294

10.1029/2003wr001981

Brunsden D. 1993. The persistence of landforms. Zeitschrift für Geomorphologie **93**: 13-28

Bull WB. 1997. Discontinuous ephemeral streams. Geomorphology **19**: 227-276

Buscombe D. 2013. Transferable wavelet method for grain-size distribution from images of sediment surfaces and thin sections, and other natural granular patterns. Sedimentology **60**: 1709-1732. DOI: 10.1111/sed.12049

Buscombe D, Rubin DM, Warrick JA. 2010. A universal approximation of grain size from images of noncohesive sediment. Journal of Geophysical Research: Earth Surface **115**: n/a-n/a. DOI: 10.1029/2009JF001477

Eaton BC, Church M. 2011. A rational sediment transport scaling relation based on dimensionless stream power. Earth Surface Processes and Landforms **36**: 901-910. DOI: 10.1002/esp.2120

Ferguson R, Hoey T, Wathen S, Werritty A. 1996. Field evidence for rapid downstream fining of river gravels through selective transport. Geology **24**: 179-182

Fryirs KA, Brierley GJ, Preston NJ, Kasai M. 2007. Buffers, barriers and blankets: The (dis)connectivity of catchment-scale sediment cascades. Catena **70**: 49-67. DOI: 10.1016/j.catena.2006.07.007

Gabet EJ, Dunne T. 2003. A stochastic sediment delivery model for a steep Mediterranean landscape. Water Resources Research **39**: 12. DOI: 1237

10.1029/2003wr002341

Goodrich DC, Keefer TO, Unkrich CL, Nichols MH, Osborn HB, Stone JJ, Smith JR. 2008. Long-term precipitation database, Walnut Gulch Experimental Watershed, Arizona, United States. Water Resources Research **44**: n/a-n/a. DOI: 10.1029/2006WR005782

Green WH, Ampt G. 1911. Studies on Soil Phyics. The Journal of Agricultural Science **4**: 1-24

Hack JT. 1957. Studies of longitudinal stream profiles in Virginia and Maryland. US Geological Survey Professional Paper 294-B: Menlo Park, CA.

Harvey AM. 2001. Coupling between hillslopes and channels in upland fluvial systems: implications for landscape sensitivity, illustrated from the Howgill Fells, northwest England. CATENA **42**: 225-250

Hassan MA. 2005. Characteristics of gravel bars in ephemeral streams. Journal of Sedimentary Research **75**: 29-42. DOI: 10.2110/jsr.2005.004

Hereford R. 2002. Valley-fill alluviation during the Little Ice Age (ca. AD 1400-1880), Paria River basin and southern Colorado Plateau, United States. Geological Society of America Bulletin **114**: 1550-1563

Jaeger K, Sutfin N, Tooth S, Michaelides K, Singer M. 2017. Geomorphology and Sediment Regimes of Intermittent Rivers and Ephemeral Streams. In *Intermittent Rivers and Ephemeral Streams*, Datry T, Bonada N, Boulton A (eds). Academic Press: Burlington; 21-49.

Korup O. 2009. Linking landslides, hillslope erosion, and landscape evolution. Earth Surface Processes and Landforms **34**: 1315-1317. DOI: 10.1002/esp.1830

Laronne JB, Reid I, Yitshak Y, Frostick LE. 1994. The non-layering of gravel streambeds under ephemeral flood regimes. Journal of Hydrology **159**: 353-363. DOI: Doi: 10.1016/0022-1694(94)90266-6

Lekach J, Schick AP. 1983. Evidence for transport of bedload in waves - analysis of fluvial sediment samples in a small upland stream channel. CATENA **10**: 267-279

Leopold LB, Bull WB. 1979. Base level, aggradation, and grade. Proceedings of the American Philosophical Society **123**: 168-202

Leopold LB, Emmett WW, Myrick RM. 1966. Hillslope Processes in a Semiarid Area New Mexico. US Geological Survey Professional Paper 352-G.

Mackin JH. 1948. Concept of the graded river. Geological Society of America Bulletin **59**: 463-512

Menting F, Langston AL, Temme AJAM. 2015. Downstream fining, selective transport, and hillslope influence on channel bed sediment in mountain streams, Colorado Front Range, USA. Geomorphology **239**: 91-105. DOI: http://dx.doi.org/10.1016/j.geomorph.2015.03.018

Michaelides K, Lister D, Wainwright J, Parsons AJ. 2009. Vegetation controls on small-scale runoff and erosion dynamics in a degrading dryland environment. Hydrological Processes **23**: 1617-1630. DOI: 10.1002/hyp.7293

Michaelides K, Lister D, Wainwright J, Parsons AJ. 2012. Linking runoff and erosion dynamics to nutrient fluxes in a degrading dryland landscape. J. Geophys. Res. **117**: G00N15. DOI: 10.1029/2012jg002071

Michaelides K, Martin GJ. 2012. Sediment transport by runoff on debris-mantled dryland hillslopes. J. Geophys. Res. **117**: F03014. DOI: 10.1029/2012jf002415

Michaelides K, Singer MB. 2014. Impact of coarse sediment supply from hillslopes to the channel in runoff-dominated, dryland fluvial systems. Journal of Geophysical Research: Earth Surface **119**: 2013JF002959. DOI: 10.1002/2013JF002959

Michaelides K, Wainwright J. 2002. Modelling the effects of hillslope-channel coupling on catchment hydrological response. Earth Surface Processes and Landforms **27**: 1441-1457. DOI: 10.1002/esp.440

Michaelides K, Wainwright J. 2008. Internal testing of a numerical model of hillslope-channel coupling using laboratory flume experiments. Hydrological Processes **22**: 2274-2291. DOI: 10.1002/hyp.6823

Michaelides K, Wilson MD. 2007. Uncertainty in predicted runoff due to patterns of spatially variable infiltration. Water Resources Research **43**:

Nearing MA, Nichols MH, Stone JJ, Renard KG, Simanton JR. 2007. Sediment yields from unit-source semiarid watersheds at Walnut Gulch. Water Resources Research **43**. DOI: 10.1029/2006wr005692

Nichols MH, Nearing MA, Polyakov VO, Stone JJ. 2013. A sediment budget for a small semiarid watershed in southeastern Arizona, USA. Geomorphology **180–181**: 137-145. DOI: http://dx.doi.org/10.1016/j.geomorph.2012.10.002

Nichols MH, Renard KG, Osborn HB. 2002. Precipitation changes from 1956 to 1996 on the Walnut Gulch Experimental Watershed. JAWRA Journal of the American Water Resources Association **38**: 161-172. DOI: 10.1111/j.1752-1688.2002.tb01543.x

Nichols MH, Stone JJ, Nearing MA. 2008. Sediment database, Walnut Gulch Experimental Watershed, Arizona, United States. Water Resources Research **44**: n/a-n/a. DOI: 10.1029/2006WR005682

Nicholson SE. 2011. Dryland Climatology. Cambridge University Press: Cambridge

Osborn HB. 1983a. Precipitation characteristics affecting hydrologic response of southwestern rangelands [USA]. United States. Dept. of Agriculture. Science and Education Administration. Western Region. Office of the Regional Administrator for Federal Research. Agricultural reviews and manuals. ARM-W (USA):

Osborn HB. 1983b. Timing and duration of high rainfall rates in the southwestern United States. Water Resources Research **19**: 1036-1042. DOI: 10.1029/WR019i004p01036

Osborn HB, Lane L. 1969. Precipitation-runoff relations for very small semiarid rangeland watersheds. Water Resources Research **5**: 419-425. DOI: 10.1029/WR005i002p00419

Parker G. 1979. Hydraulic geometry of active gravel rivers. Journal of the Hydraulics Division **105**: 1185-1201

Pelletier JD, DeLong S. 2004. Oscillations in arid alluvial-channel geometry. Geology **32**: 713-716. DOI: 10.1130/g20512.1

Powell DM, Brazier R, Parsons A, Wainwright J, Nichols M. 2007. Sediment transfer and storage in dryland headwater streams. Geomorphology **88**: 152-166. DOI: http://dx.doi.org/10.1016/j.geomorph.2006.11.001

Powell DM, Laronne JB, Reid I, Barzilai R. 2012. The bed morphology of upland single-thread channels in semi-arid environments: evidence of repeating bedforms

and their wider implications for gravel-bed rivers. Earth Surface Processes and Landforms **37**: 741-753. DOI: 10.1002/esp.3199

Renard KG, Keppel RV. 1966. Hydrographs of ephemeral streams in the Southwest. Journal of the Hydraulics Division-Asce **92**: 33-52

Renard KG, Laursen EM. 1975. Dynamic behavior model of ephemeral stream. Journal of the Hydraulics Division **101**: 511-528

Rice S, Church M. 1996. Bed material texture in low order streams on the Queen Charlotte Islands, British Columbia. Earth Surface Processes and Landforms **21**: 1-18. DOI: 10.1002/(sici)1096-9837(199601)21:1<1::aid-esp506>3.0.co;2-f

Simpson G, Schlunegger F. 2003. Topographic evolution and morphology of surfaces evolving in response to coupled fluvial and hillslope sediment transport. Journal of Geophysical Research: Solid Earth **108**: n/a-n/a. DOI: 10.1029/2002JB002162

Singer MB. 2010. Transient response in longitudinal grain size to reduced gravel supply in a large river. Geophysical Research Letters **37**: L18403, doi:10.1029/2010gl044381. DOI: 10.1029/2010gl044381

Singer MB, Michaelides K. 2014. How is topographic simplicity maintained in ephemeral dryland channels? Geology **42**: 1091-1094. DOI: 10.1130/g36267.1

Singer MB, Michaelides K. 2017. Deciphering the expression of climate change within the Lower Colorado River basin by stochastic simulation of convective rainfall. Environmental Research Letters **12**. DOI: 10.1088/1748-9326/aa8e50

Sklar LS, Riebe CS, Marshall JA, Genetti J, Leclere S, Lukens CL, Merces V. 2017. The problem of predicting the size distribution of sediment supplied by hillslopes to rivers. Geomorphology **277**: 31-49. DOI: https://doi.org/10.1016/j.geomorph.2016.05.005

Slater LJ, Singer MB. 2013. Imprint of climate and climate change in alluvial riverbeds: Continental United States, 1950-2011. Geology **41**: 595-598. DOI: 10.1130/g34070.1

Slater LJ, Singer MB, Kirchner JW. 2015. Hydrologic versus geomorphic drivers of trends in flood hazard. Geophysical Research Letters: 2014GL062482. DOI: 10.1002/2014GL062482

Snow RS, Slingerland RL. 1987. Mathematical-modeling of graded river profiles. Journal of Geology **95**: 15-33

Sternberg H. 1875. Untersuchungen über längen-und Querprofil geschiebeführender Flüsse. publisher not identified

Stone JJ, Nichols MH, Goodrich DC, Buono J. 2008. Long-term runoff database, Walnut Gulch Experimental Watershed, Arizona, United States. Water Resources Research **44**. DOI: 10.1029/2006wr005733

Syed K, Goodrich DC, Myers D, Sorooshian S. 2003. Spatial characteristics of thunderstorm rainfall fields and their relation to runoff. Journal of Hydrology **271**: 1-21. DOI: 10.1016/S0022-1694(02)00311-6

Tucker GE, Bras RL. 1998. Hillslope processes, drainage density, and landscape morphology. Water Resources Research **34**: 2751-2764

Tucker GE, Slingerland R. 1997. Drainage basin responses to climate change. Water Resources Research **33**: 2031-2047. DOI: 10.1029/97WR00409

Vogel JC. 1989. Evidence of past climatic change in the Namib Desert. Palaeogeography, Palaeoclimatology, Palaeoecology **70**: 355-366. DOI: http://dx.doi.org/10.1016/0031-0182(89)90113-2

Wainwright J, Calvo Cases A, Puigdefábregas J, Michaelides K. 2002. Editorial. Earth Surface Processes and Landforms **27**: 1363-1364. DOI: 10.1002/esp.434

Walling DE, Fang D. 2003. Recent trends in the suspended sediment loads of the world's rivers. Global and Planetary Change **39**: 111-126. DOI: http://dx.doi.org/10.1016/S0921-8181(03)00020-1

Waters MR, Haynes CV. 2001. Late Quaternary arroyo formation and climate change in the American Southwest. Geology **29**: 399-402

Willgoose G, Bras RL, Rodriguez-Iturbe I. 1991. A coupled channel network growth and hillslope evolution model: 1. Theory. Water Resources Research **27**: 1671-1684. DOI: 10.1029/91WR00935

Wolman MG. 1954. A method of sampling coarse river-bed material. EOS, Transactions American Geophysical Union **35**: 951-956

Wolman MG, Gerson R. 1978. Relative time scales of time and effectiveness of climate in watershed geomorphology. Earth Surface Processes & Landforms **3**: 189-208

Wolman MG, Miller JP. 1960. Magnitude and frequency of forces in geomorphic processes. Journal of Geology **68**: 54-74

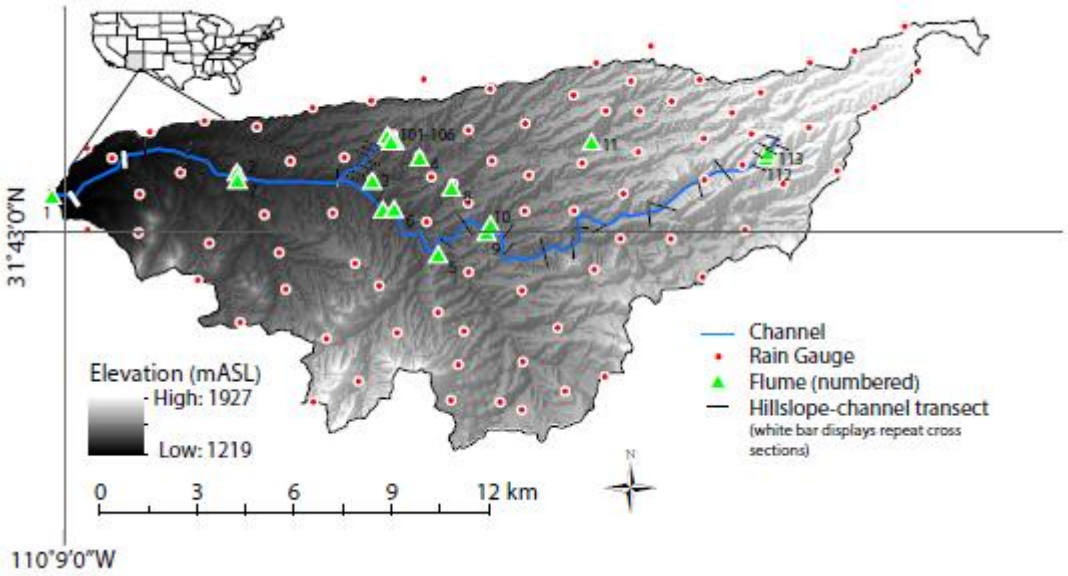

Figure 1. Walnut Gulch Experimental Watershed near Tombstone, Arizona, USA showing locations of hillslope- channel transects, rain gauges and channel flumes. Base map data source: USGS 10m DEM.

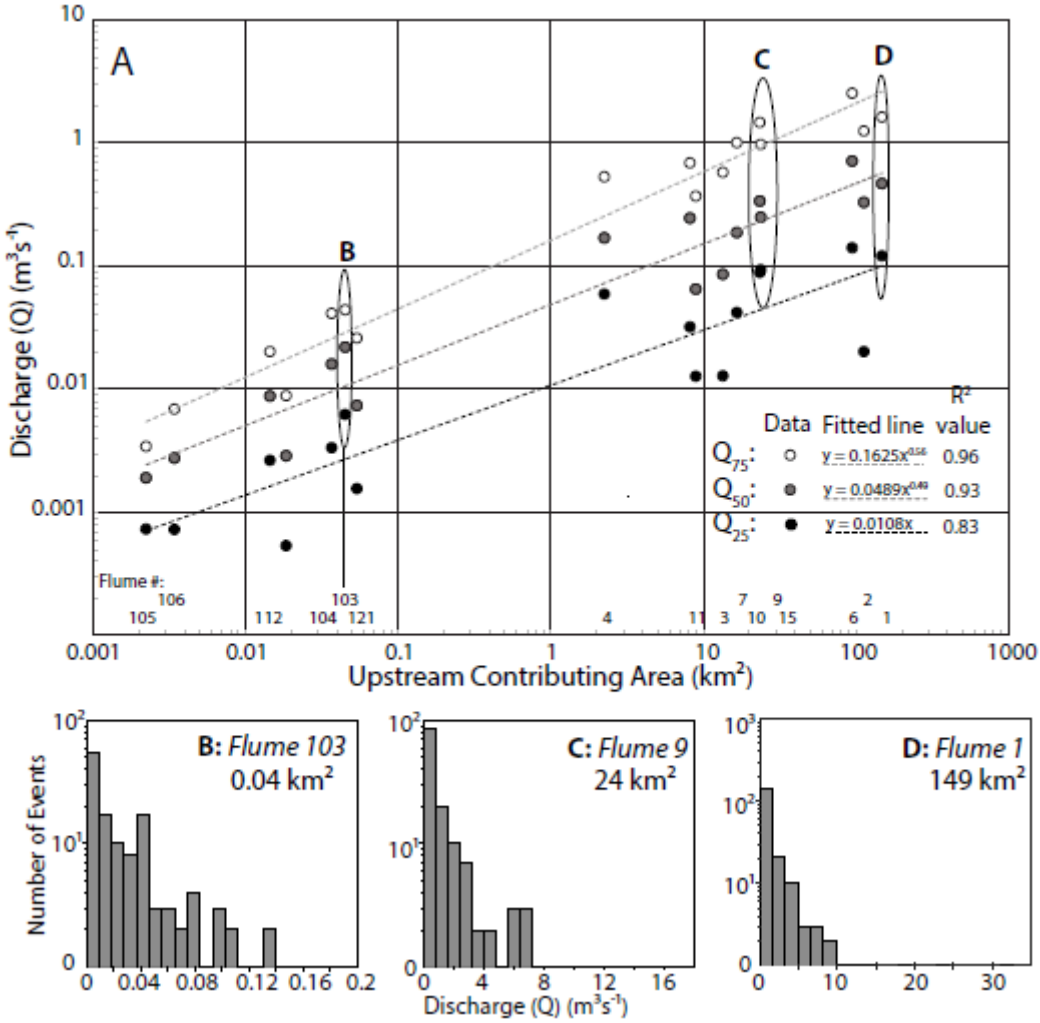

Figure 2. A) Discharge (Q) at 25th (black), 50th (grey) and 75th (white) percentiles at all channel flumes within Walnut Gulch Experimental Watershed, plotted against upstream contributing area (determined from Lidar). Q values were available for 14 sub-watersheds of varying areas within the basin (numbered in A and keyed to Figure 1). Histograms of discharge events for the three ovaled watersheds in A: a small watershed, Flume 103 (B), a medium-sized watershed, Flume 9 (C), a large watershed, Flume1 (D). Note: scales on x-axes differ between subplots.

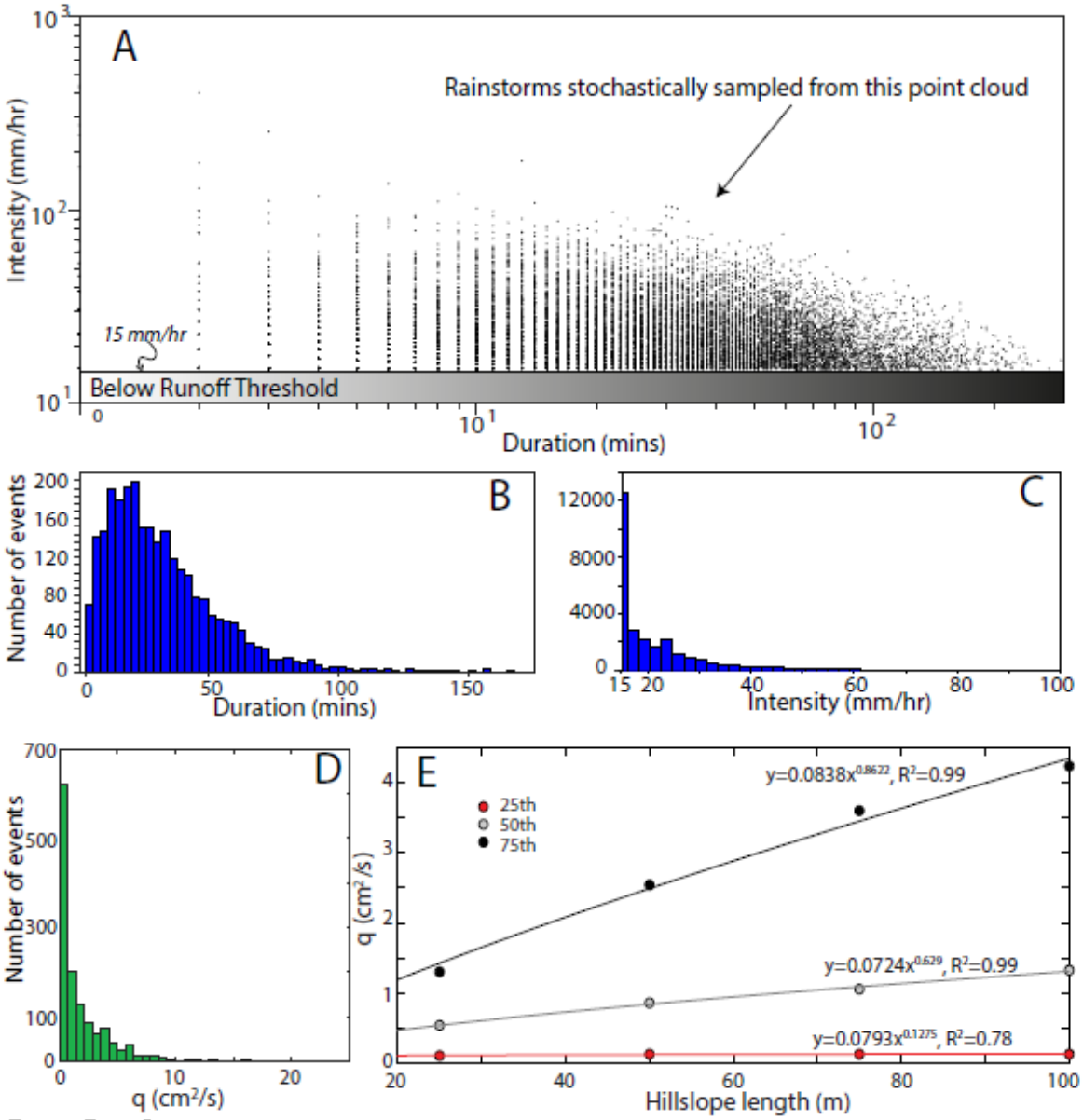

Figure 3. A) Phase space of rainfall intensity versus duration. These data were thresholded at 15 mm/hr, for all data measured at WGEW since 1953 (black dots). We sampled from this distribution and then used these data to drive COUP2D. B) Histogram of all rainfall durations for storm events > 15 mm/hr and the quartile values for the distribution. C) Histogram of rainfall intensities for rainfall events >15 mm/hr and the extracted intensities for each curve in (A). D) Histogram of all modelled hillslope runoff (n=1832), based on stochastic simulation of runoff on slopes of 4 different lengths. E) Relationships between hillslope length and the q percentiles of modelled runoff used later to calculate the q percentiles for the measured hillslopes in WGEW.

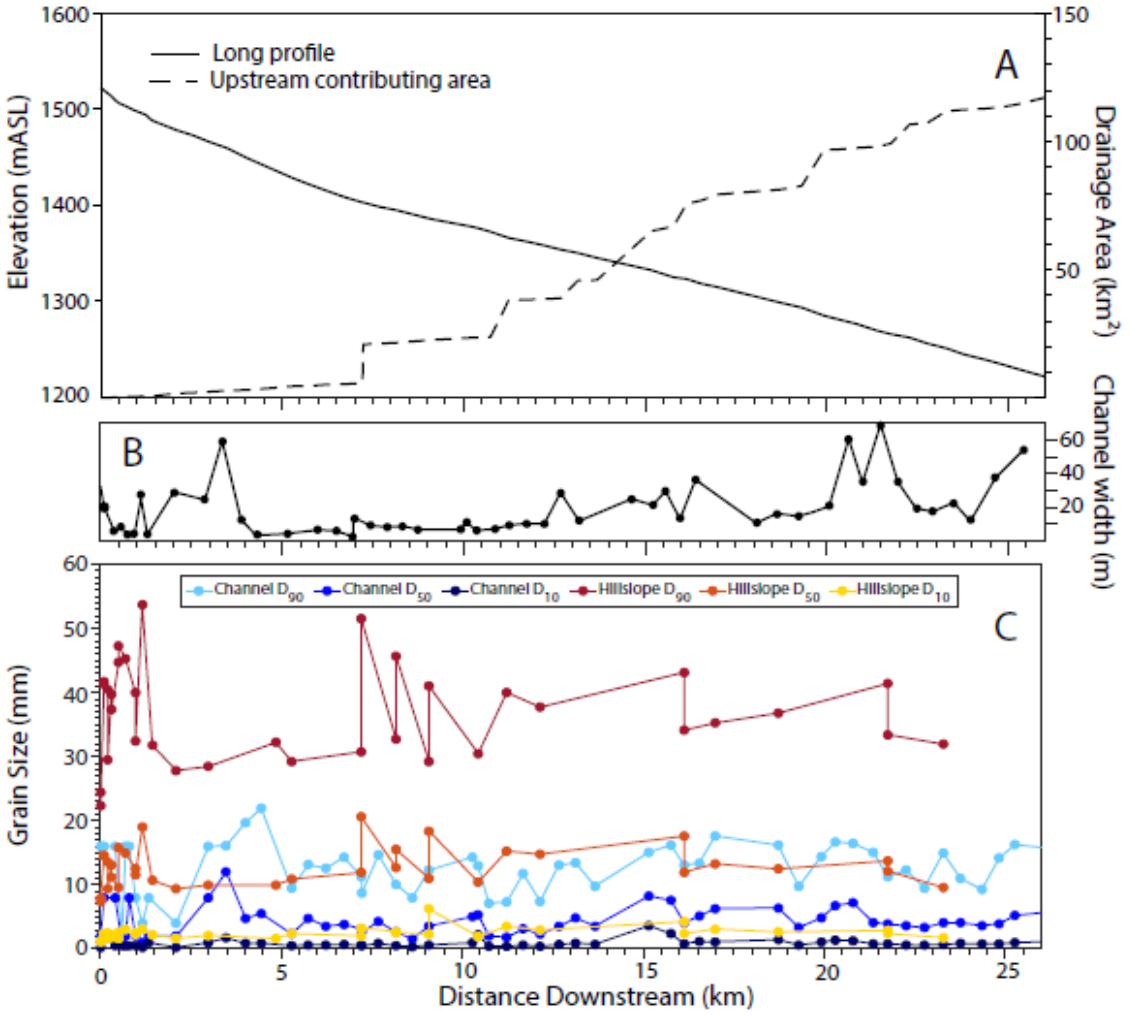

Figure 4. A) Longitudinal profile and corresponding drainage area, B) channel width and C) characteristic grain sizes on hillslopes and in the channel. There is a statistical similarity between hillslope D_{50} and channel D_{90} (Kolmogorov-Smirnov statistic = 0.18, p = 0.28, n1/n2 = 72/31).

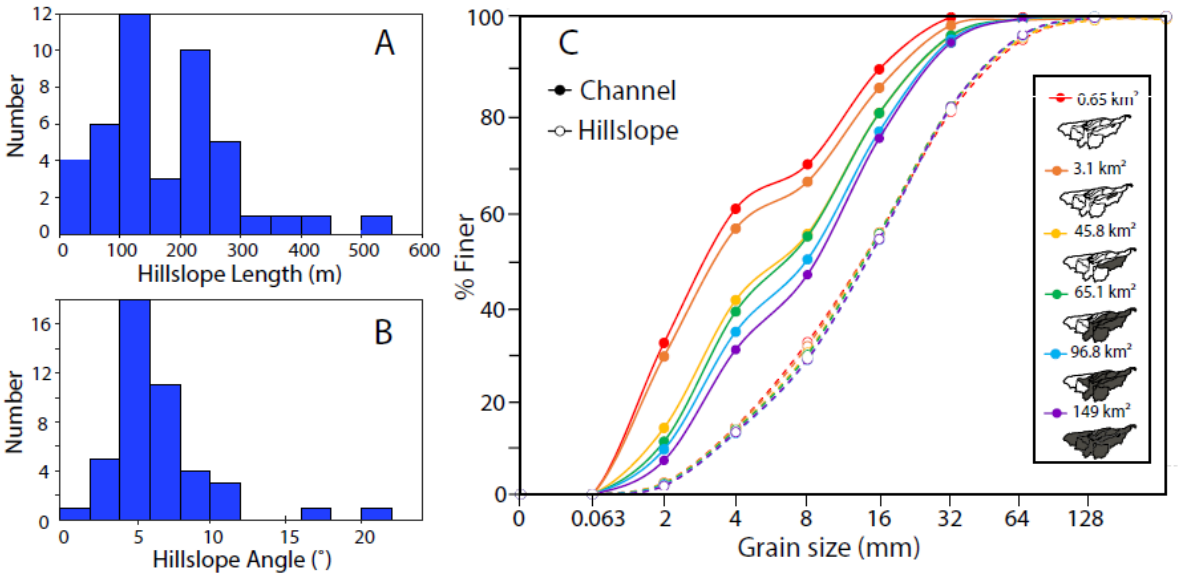

Figure 5. Field Data: Histograms of hillslope lengths (A) and angles (B) measured in WGEW, and the aggregated GSDs downstream for all channel locations (solid line with filled symbols) and hillslopes (dashed lines with open symbols) within each colour-coded nested watershed area (C).

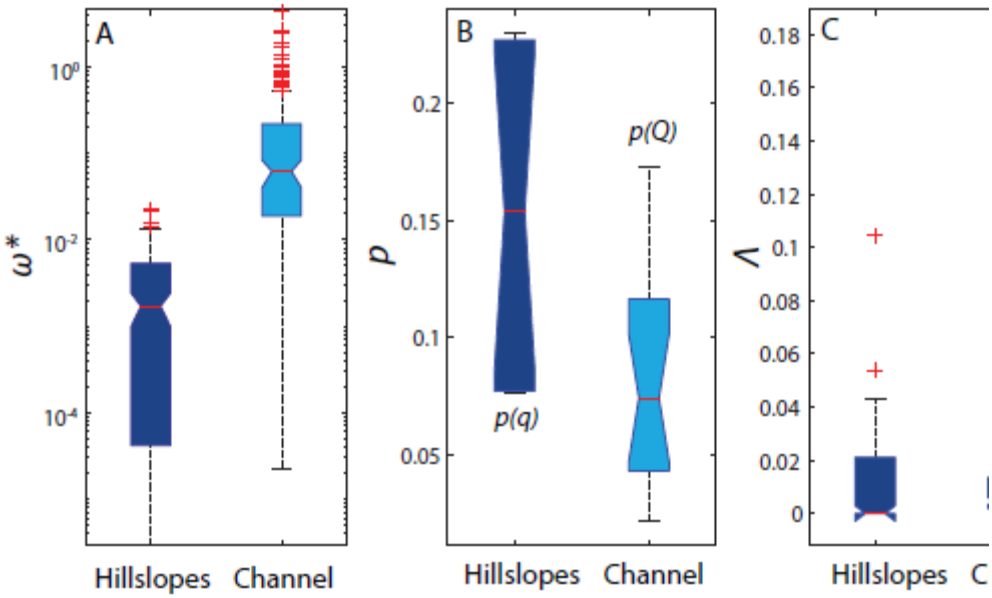

Figure 6. A: Box and whisker plots displaying the median and inter quartile range of dimensionless stream power, ω^*, B: Probability of occurrence, p, C: The product of dimensionless stream power and the probability of occurrence, Λ, for hillslopes and channel locations in WGEW.

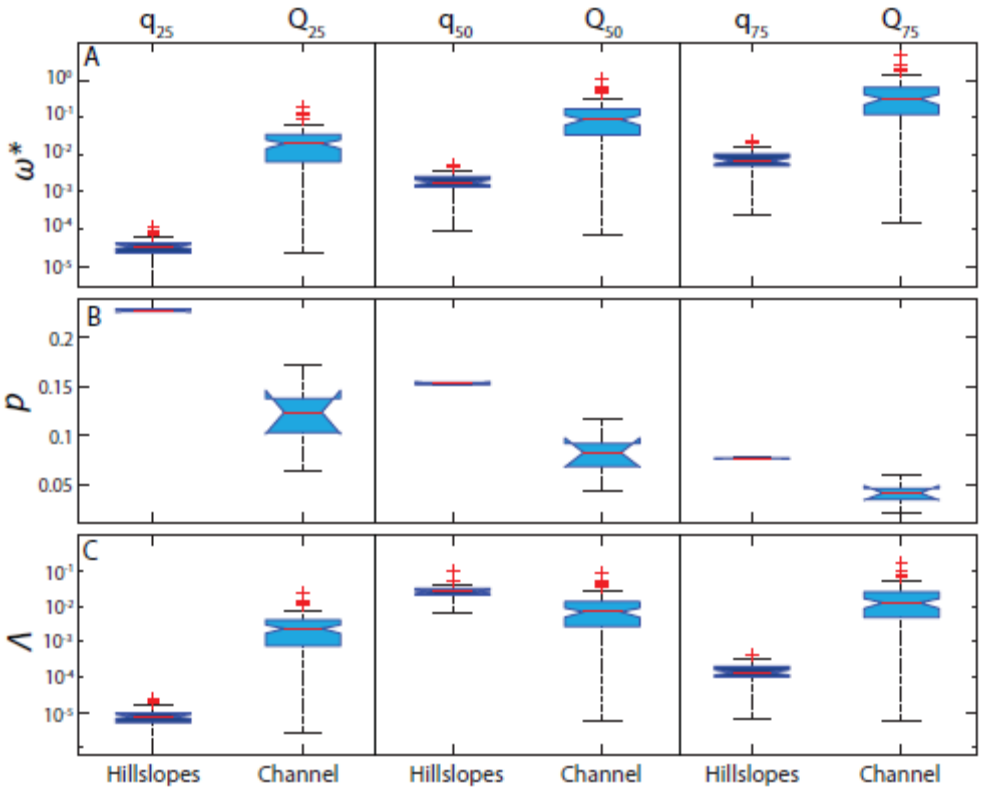

Figure 7. Box and whisker plots displaying the median and inter quartile range for dimensionless stream power, ω^* (A), probability of occurrence, p (B) and their product Λ (C) at each percentile of flow used in this study. Data are grouped by hillslopes and channels.

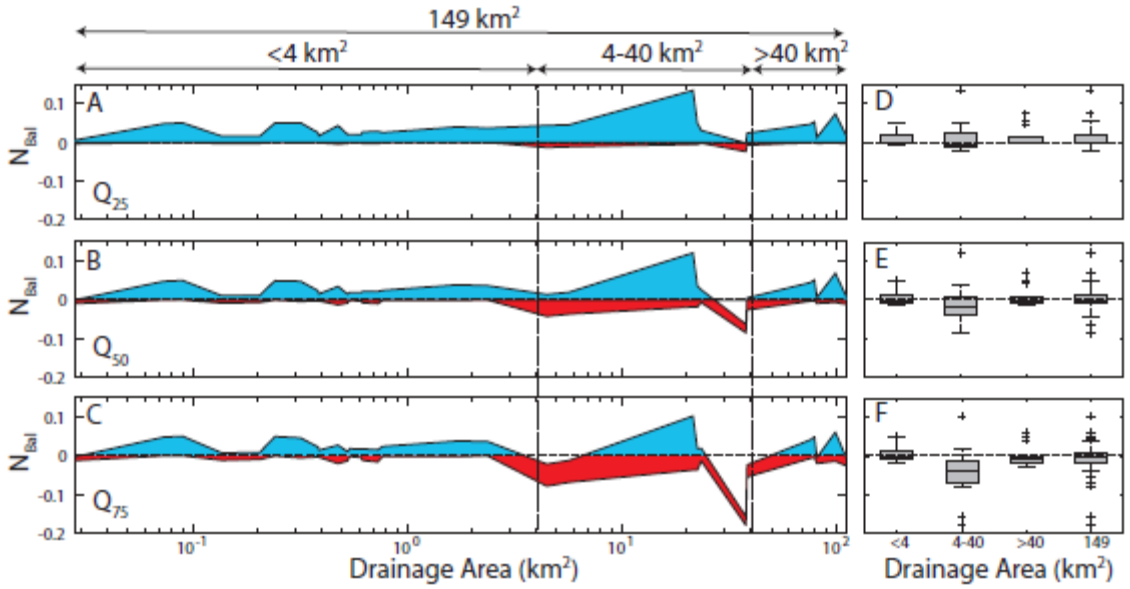

Figure 8. Spatial plots of net balance of Λ values (N_{Bal}) for fixed percentiles of Q (A-C). Variability is defined by the range of hillslope q. Positive values are shown in blue and negative in red. Panels D-F show box and whisker plots of aggregated values of N_{Bal} for various spatial scales.

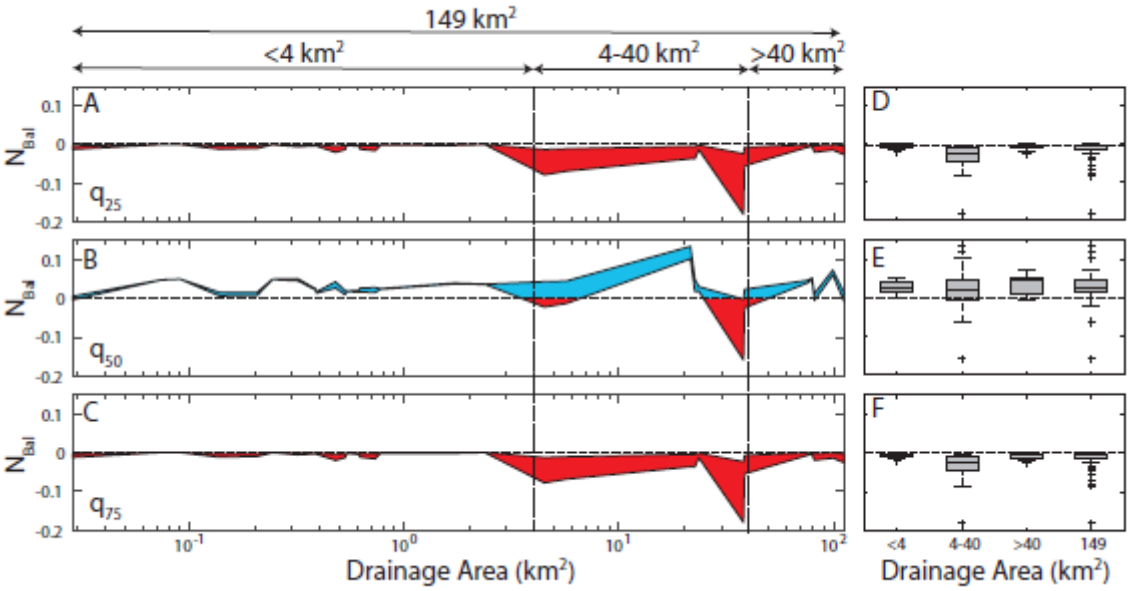

Figure 9. Spatial plots of net balance of Λ values (N_{Bal}) for fixed percentiles of q (A-C). Variability is defined by the range of channel Q. Positive values are shown in blue and negative in red. Panels D- F show box and whisker plots of aggregated values of N_{Bal} for various spatial scales.

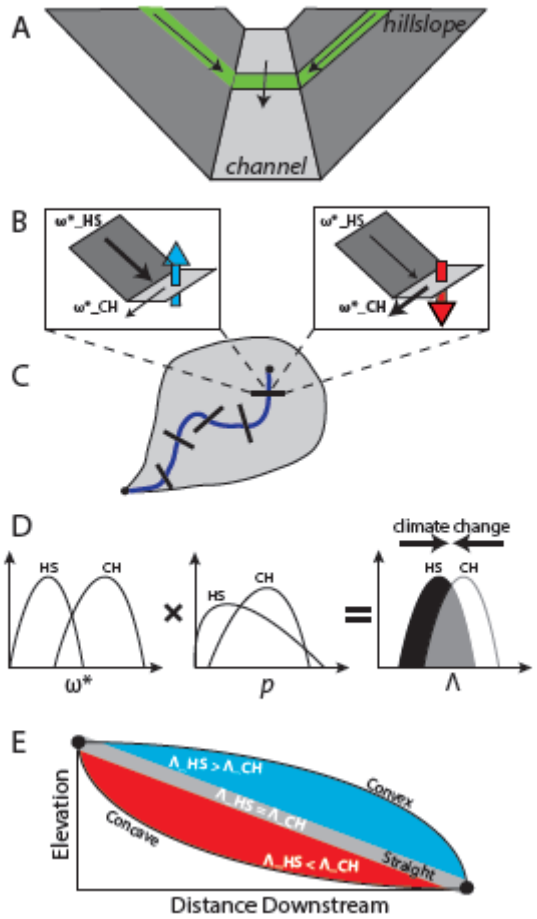

Figure 10. A schematic of the framework set out in this study. At hillslope-channel transects (A) we assess the net balance of ω^* as a proxy for sediment transport (B). If the stream power in the channel is greater than the stream power on the hillslope, then the channel bed will degrade, and vice versa. We assess the net balance at transects throughout the basin (C). Our framework includes the calculation of ω^*, the frequency of occurrence of corresponding flows, p, and the product of these, Λ, to assemble pdfs of net balance over a multi-decadal time period (D). When the net balance, between Λ_HS and Λ_CH is positive, the longitudinal profile will tend toward convex up and vice versa (E). In drylands, however, straight profiles are often observed, suggesting zero N_{Bal}. Climate changes that differentially alter runoff regimes on slopes and in the channel, can change this balance. At Walnut Gulch, lower rainfall intensity favouring more storms would shift lambda distributions closer together (D), reinforcing a zero N_{Bal}.